1 **Metabolic disruption impacts tick fitness and microbial relationships**

2

3 **Authors:** Sourabh Samaddar[1], Anya J. O'Neal[1], Liron Marnin[#1], Agustin Rolandelli[#1], Nisha

4 Singh[1], Xiaowei Wang[1†], L. Rainer Butler[1], Parisa Rangghran[2], Hanna J. Laukaitis[1], Francy E.

5 Cabrera Paz[1], Gary M. Fiskum[2], Brian M. Polster[2] and Joao H. F. Pedra[1*]

6

7 **Affiliations:** [1]Department of Microbiology and Immunology, University of Maryland, School of

8 Medicine, Baltimore, Maryland 21201, USA

9 [2]Department of Anesthesiology and Center for Shock, Trauma and Anesthesiology Research,

10 School of Medicine, University of Maryland, Baltimore, MD 21201, USA

11 [#]Contributed equally.

12

13 [†]Present address: MP Biomedicals, Solon, Ohio 44139, USA

14 *Corresponding Author: jpedra@som.umaryland.edu

15

16 **Keywords:** Vector-Borne Diseases, Ticks, *Borrelia burgdorferi*, Lyme Disease, Rickettsial

17 Infection, Metabolism

Abstract

18

19   Arthropod-borne microbes rely on the metabolic state of a host to cycle between

20   evolutionarily distant species. For instance, arthropod tolerance to infection may be due to

21   redistribution of metabolic resources, often leading to microbial transmission to mammals.

22   Conversely, metabolic alterations aids in pathogen elimination in humans, who

23   do not ordinarily harbor arthropod-borne microbes. To ascertain the effect of metabolism on

24   interspecies relationships, we engineered a system to evaluate glycolysis and oxidative

25   phosphorylation in the tick *Ixodes scapularis*. Using a metabolic flux assay, we determined that

26   the rickettsial bacterium *Anaplasma phagocytophilum* and the Lyme disease spirochete *Borrelia*

27   *burgdorferi*, which are transstadially transmitted in nature, induced glycolysis in ticks. On the

28   other hand, the endosymbiont *Rickettsia buchneri,* which is transovarially maintained, had a

29   minimal effect on *I. scapularis* bioenergetics. Importantly, the metabolite β-aminoisobutyric acid

30   (BAIBA) was elevated during *A. phagocytophilum* infection of tick cells following an unbiased

31   metabolomics approach. Thus, we manipulated the expression of genes associated with the

32   catabolism and anabolism of BAIBA in *I. scapularis* and detected impaired feeding on

33   mammals, reduced bacterial acquisition, and decreased tick survival. Collectively, we reveal the

34   importance of metabolism for tick-microbe relationships and unveil a valuable metabolite for *I.*

35   *scapularis* fitness.

Introduction

36

37   Arthropod-borne microbes contribute to the global disease burden and are responsible

38   for hundreds of millions of human infections each year[1]. In the United States, the deer tick

39   *Ixodes scapularis* is the predominant arthropod vector and is responsible for transmitting several

40   known human pathogens, including the Lyme disease spirochete *Borrelia burgdorferi* and the

41   obligate intracellular rickettsial bacterium *Anaplasma phagocytophilum* that causes human

42   granulocytic anaplasmosis[2-4]. Although these microbes are best characterized for their ability to

43   cause disease in humans, our knowledge related to the associations between ticks and

44   microbes remains rudimentary. For instance*, I. scapularis* readily acquires *B. burgdorferi* and *A.*

45   *phagocytophilum* and tolerates their presence transstadially, or throughout developmental

46   stages, but does not transmit to new progeny[5]. On the other hand, *I. scapularis* possesses

47   endosymbiotic bacteria, primarily *Rickettsia buchneri*, that are vertically transmitted from female

48   to progeny but are considered non-pathogenic to humans[6-8]. Overall, tick-microbe relationships

49   are maintained by balancing immune and metabolic responses[9-12] with fitness advantages

50   conferred by some intracellular bacteria[13-15].

51   Parasitism results in a significant fitness cost to the host, such as weight loss, reduced

52   survival or impaired reproductive capacity[16,17]. Thus, a host may redistribute finite resources

53   upon infection to balance life history programs, including maintenance, growth and

54   reproduction[17-20]. This redistribution, also known as resource allocation, is a main driver in the

55   organism's response to unfavorable conditions (*e.g.*, pathogen infection) and the push towards

56   maintenance strategies[21,22]. An example of a maintenance strategy within the cell is metabolic

57   reprogramming, where immune and cancer cells shift their metabolism to aerobic glycolysis,

58   also known as the Warburg effect[23], to sustain proliferation and/or immune effector

59   functions[22,24,25]. Metabolic reprogramming and resource allocation have been largely studied

60   through the lens of evolutionary ecology and mammalian biology[21,22,24-30]. However, the

61   metabolic contribution to vector competence remains largely undefined[11,12,31] despite the unique

62   biological relationships between arthropods and the microbes they carry. Previous work

63   suggested that *A. phagocytophilum* and *B. burgdorferi* influence the metabolism of ticks[10,32-38].

64   Unfortunately, how disruptions in bioenergetic processes affect ticks on a cellular or systemic

65   level remains fragmented. Furthermore, in what manner ticks respond metabolically to

66   transstadially-infected microbes that cause human diseases compared to a transovarially

67   maintained endosymbiont remain obscure. Finally, individual metabolites that contribute to tick

68   fitness and bacterial acquisition are mostly undetermined.

69   In this study, we sought to develop a platform for studying bioenergetics in *I. scapularis*.

70   We established a system for manipulating glycolysis and oxidative phosphorylation (OxPhos) in

71   tick cells and measured how disruption in bioenergetic processes affected arthropod fitness. We

72   undertook an unbiased metabolomics approach to characterize metabolic signatures in tick cells

73   infected with either the human pathogen *A. phagocytophilum*[4] or the endosymbiont *R. buchneri*[6-

74   8]. We identified a key metabolite in ticks, β-aminoisobutyric acid (BAIBA), that is elevated by *A.*

75   *phagocytophilum*. Finally, we demonstrated that manipulation of gene expression related to the

76   catabolism and anabolism of the D-BAIBA enantiomer in *I. scapularis* influences both tick fitness

77   and bacterial acquisition.

Results

Establishment of a system to measure bioenergetics in ticks. Glycolysis, which takes place in the cytoplasm and leads to the production of lactate, and OxPhos, which occurs in the mitochondria and utilizes the electron transport chain (ETC), provides energy for metabolic processes within cells through the generation of adenosine triphosphate (ATP)[22,24,25,30]. Glycolysis and OxPhos can be measured by analyzing the extracellular acidification rate (ECAR) and oxygen consumption rate (OCR), respectively[39]. In the mammalian literature, these processes are evaluated using the Seahorse metabolic flux assay[40], where cellular metabolism is manipulated by small molecule inhibitors that block enzymatic function. For example, 2-deoxy D-glucose (2-DG) inhibits hexokinase activity, the rate-limiting enzyme in glycolysis, while rotenone, antimycin A, oligomycin, and 2,4-dinitrophenol (2,4-DNP) hinder mitochondrial OxPhos[22,24,25,30] (Fig. 1A).

We created a modified version of the commonly used L15C300 medium to culture tick cells (referred to as mL15C)[41] (table S1), which supports the growth of *I. scapularis* ISE6 cells in the presence of glycolytic and OxPhos molecular inhibitors for at least 48 hours (Figs. 1B-F; fig. S1). Other tick cells available within the scientific community, including IDE12 (*I. scapularis*), AAE2 (*Amblyomma americanum*) and DAE100 (*Dermacentor andersoni*) were not permissive to biochemical manipulation in culture (fig. S2). Thus, we used the *I. scapularis* ISE6 cells for a metabolic flux assay. Using the Seahorse analyzer with drug concentrations that did not affect viability, we demonstrated that ECAR and OCR can be measured in live *I. scapularis* cells (Figs. 1G-H). The addition of glucose led to enhanced extracellular acidification in the mL15C medium containing ISE6 cells (Fig. 1G). The subsequent addition of 2-DG to inhibit hexokinase activity returned extracellular acidification to background levels (Fig. 1G). We also observed an increase in the oxygen consumption rate within *I. scapularis* ISE6 cells upon adding the 2,4-DNP uncoupler. The 2,4-DNP uncoupler disrupts the electrochemical gradient across the mitochondrial inner membrane (Fig. 1H). We decreased the electron transport flow in

5

104   mitochondria with rotenone (Complex I inhibitor) and antimycin A (Complex III inhibitor), which

105   resulted in reduction of cellular respiration (Fig. 1H). Altogether, we were able to measure

106   critical bioenergetic functions in tick cells, including glycolysis and mitochondrial respiration.

107   In a tick life cycle, growth is influenced by the uptake of a blood meal and can be directly

108   measured by weight, which is dependent on attachment to mammals. Alternatively,

109   maintenance can be assessed by tick survival and molting to subsequent developmental

110   stages. To determine how metabolic inhibitors influenced ticks *in vivo*, we then injected nymphs

111   with distinct amounts of 2-DG or oligomycin and measured fitness parameters, including

112   attachment, feeding, survival, and molting. For the 2-DG treatment, we observed a dose-

113   dependent effect on tick attachment, but we did not detect differences in other aspects of tick

114   fitness (Fig. 1I and fig. S3). Conversely, elevated concentrations of oligomycin reduced survival

115   in unfed nymphs (fig. S4A). Based on this information, we used an intermediate oligomycin

116   amount (0.8 pmol) in subsequent experiments to measure fitness parameters in fed ticks.

117   Interestingly, we observed a significant reduction in the molting capacity of ticks injected with

118   oligomycin. All *I. scapularis* injected with the vehicle control phosphate-buffered saline (PBS)

119   molted to adults within 120 days post-feeding on mice (Figs. 1J-K). On the other hand, only 36%

120   of nymphs injected with oligomycin molted during this time period (Figs. 1J-K). Chemical

121   inhibition of the OxPhos complex V by oligomycin did not impair attachment, weight, or survival

122   in fed nymphs (figs. S4B-D). Collectively, our results indicated that oligomycin has distinct

123   effects on fed versus unfed *I. scapularis* nymphs. Furthermore, inhibitors of glycolysis and

124   OxPhos altered biological programs associated with tick growth and maintenance.

125

126   ***A. phagocytophilum* and *B. burgdorferi* increase glycolysis in tick cells compared**

127   **to the endosymbiont *R. buchneri*.** During an infection, the host switches its metabolism to

128   glycolysis to fuel immune cells and respond to cellular stress[42,43]. Conversely, pathogenic

129   microbes upregulate glycolysis to establish infection and turn on virulence programs[22,42]. We

130   aimed to characterize the tick metabolic response during microbial stimulation. *I. scapularis* may

131   carry *A. phagocytophilum* and *B. burgdorferi*, two bacterial pathogens that are transstadially

132   transmitted[2-4]. Furthermore, they harbor the endosymbiont *R. buchneri*, which is non-pathogenic

133   to humans and passed transovarially to other ticks[6]. Thus, we measured glycolysis (ECAR) and

134   OxPhos (OCR) in tick cells infected with *A. phagocytophilum*, *B. burgdorferi*, or *R. buchneri* (Fig.

135   2A). After 48 hours of culturing *I. scapularis* ISE6 cells in the mL15C medium, *A.*

136   *phagocytophilum* or *B. burgdorferi*, but not *R. buchneri*, upregulated glycolysis in a manner

137   consistent with the multiplicity of infection (MOI) (Fig. 2B-D). This glycolytic effect on tick cells

138   was more pronounced when glucose was added to the medium culture (Fig. 2B-D). Importantly,

139   we did not observe any noteworthy impact of bacterial MOI for OxPhos across all conditions

140   based on the OCR analysis (Fig. 2E-G).

141   We then validated the Seahorse metabolic flux assay through colorimetric assays (Fig.

142   3A). Infection of tick cells with the human pathogens *A. phagocytophilum* or *B. burgdorferi*

143   resulted in increased activity of the enzymes phosphoglucose isomerase (PGI) and lactate

144   dehydrogenase (LDH) (Fig. 3B and 3C, 3E and 3F). Similarly, we observed higher

145   concentrations of lactate after 1 and 24 hours and decreased concentrations of NADH at 24

146   hours (Fig. 3H and 3I, 3K and 3L). On the other hand, infection of tick cells with *R. buchneri* did

147   not result in significant changes in glycolytic enzymatic activity (Fig. 3D and 3G), although we

148   measured slightly increased levels of lactate and decreased NADH at 24 hours, respectively

149   (Fig. 3J and 3M).

150   We did not observe metabolic changes in components of the tricarboxylic acid (TCA)

151   cycle upon *A. phagocytophilum* infection, as measured by the enzymatic activities of aconitase

152   and succinate dehydrogenase and the metabolites citrate and succinate, respectively (fig. S5).

153   These findings suggested that interactions between tick cells and the human pathogens *A.*

154   *phagocytophilum* and *B. burgdorferi* affect glycolysis in *I. scapularis* cells. Furthermore, bacterial

7

155   associations occurring upon *A. phagocytophilum* and *B. burgdorferi* infection of tick cells are

156   distinct from those of the endosymbiont *R. buchneri*.

157

158   **Infection with the human pathogen *A. phagocytophilum* alters the metabolism of**

159   **tick cells compared to the endosymbiont *R. buchneri*.** We then tested whether distinct

160   metabolic states (*e.g.*, glycolysis or OxPhos) affected bacterial burden in tick cells. We pre-

161   treated *I. scapularis* ISE6 cells cultured in the mL15C medium with oligomycin, 2,4-DNP,

162   rotenone, antimycin A or 2-DG and measured microbial infection 48 hours later (Fig. 4A). We

163   observed that inhibiting glycolysis with 2-DG had no significant effect on bacterial burden in

164   ISE6 cells (Figs. 4B and 4C). However, impairing OxPhos with oligomycin, rotenone or

165   antimycin A led to a pronounced increase in *A. phagocytophilum* infection of tick cells (Fig. 4B).

166   Comparatively, only a modest increase in *R. buchneri* infection was noted after blocking

167   OxPhos (Fig. 4C). Importantly, treatment of tick cells with the uncoupler 2,4-DNP neither

168   affected *A. phagocytophilum* nor *R. buchneri* infection (Fig. 4B and 4C). Overall, these results

169   indicated that impeding OxPhos in tick cells created an environment that benefited *A.*

170   *phagocytophilum*, and to a lesser extent, *R. buchneri*.

171   Given the results obtained for *A. phagocytophilum* and *R. buchneri* infection, we posited

172   that these two obligate intracellular bacteria induced contrasting metabolic responses in *I.*

173   *scapularis*. Hence, *I. scapularis* ISE6 cells were infected with either *A. phagocytophilum* or *R.*

174   *buchneri* at indicated time points followed by an unbiased metabolomics analysis (Fig. S6) [data

175   available via MetaboLights, identifier MTBLS686]. Metabolite levels were globally increased

176   upon *A. phagocytophilum* infection, whereas *R. buchneri* contributed to fewer metabolic

177   changes. Using a pathway enrichment analysis, we observed significant alterations in energy

178   metabolites (figs. S7 and S8), nucleotide (figs. S9 and S10), fatty acid (figs. S11 and S12),

179   methionine (figs. S13 and S14), protein degradation (figs. S15 and S16) and membrane lipid

180   metabolism (fig. S17) upon *A. phagocytophilum* infection of *I. scapularis* ISE6 compared to *R.*

8

181   *buchneri*. We concluded that *A. phagocytophilum* affects the metabolism of tick cells to a

182   greater extent than the bacterial symbiont *R. buchneri*.

183

184   **D-β-aminoisobutyric acid (D-BAIBA) affects *A. phagocytophilum* acquisition in**

185   **ticks.** Next, we wanted to functionally characterize these pathways *in vivo* to demonstrate the

186   utility of the metabolomics dataset for tick-microbe relationships. As described in the

187   metabolomics analysis (figs. S6-S17), we determined that fatty acid, lipid and nucleotide

188   metabolism in tick cells were impacted by *A. phagocytophilum* infection. Therefore, we focused

189   our efforts on a pleiotropic metabolite that was involved in these processes. β-aminoisobutyric

190   acid (BAIBA) is an intermediate of nucleotide and amino acid metabolism[44,45]. BAIBA is also

191   associated with fatty acid β-oxidation, lipid homeostasis and the browning of white adipose

192   tissue in mammals[44,45]. BAIBA has two enantiomers, D-BAIBA and L-BAIBA, that are generated

193   by different enzymatic processes. During thymine degradation, N-carbamoyl BAIBA is converted

194   to D-BAIBA by the enzyme β-ureidopropionase 1 (UPB1) before being catabolized to D-

195   methylmalonate semialdehyde by alanine-glyoxylate aminotransferase 2 (AGXT2). Alternatively,

196   L-BAIBA is a byproduct of L-valine catabolism and is generated by the enzyme 4-aminobutyrate

197   aminotransferase (ABAT) through a reversible reaction from L-methylmalonate semialdehyde[45].

198   Both forms are eventually converted into propionyl-CoA, which funnels into the TCA cycle as a

199   succinyl-CoA metabolite (Fig. 4D).

200   BAIBA was significantly elevated 24 hours after *A. phagocytophilum* infection compared

201   to *R. buchneri* in *I. scapularis* ISE6 cells (Fig. 4E). Importantly, our metabolomics data did not

202   distinguish between BAIBA enantiomers. Thus, we reconstructed the BAIBA pathway *in silico*

203   and identified the ortholog genes in *I. scapularis* ticks for catabolism and anabolism: (*upb1*)

204   [XM_029991952.1], (*agxt2*) [XM_029990918.1] and (*abat*) [XM_002405926.2] (Fig. 4D and

205   table S2). We observed that ticks fed on *A. phagocytophilum*-infected mice upregulated the

9

206   expression of *upb1* and *agxt2*, but not *abat* (Figs. 4F-H). Therefore, we characterized the impact

207   of D-BAIBA regulation in tick-microbe interactions by manipulating the gene expression of *upb1*

208   and *agxt2*. We silenced *upb1* or *agxt2* expression in ticks using small interfering RNAs (siRNAs)

209   (Figs. 4I and 4K). RNAi remains the gold standard for disruption of tick proteins associated with

210   biochemical pathways, as genome editing through clustered regularly interspaced short

211   palindromic repeats (CRISPR) has only been applied to appendage genes to score

212   morphological phenotypes[46]. *upb1-* or *agxt2*-silenced ticks fed on *A. phagocytophilum*-infected

213   mice acquired significantly fewer bacteria than the control treatment (Figs. 4J and 4L). Then, we

214   performed an experiment to determine whether the addition of exogenous BAIBA in ticks affects

215   bacterial acquisition. We injected ticks with a racemic mixture of BAIBA and an isomer (α-

216   aminoisobutyric acid) before placing these ectoparasites on mice infected with *A.*

217   *phagocytophilum*. As shown in Figs. 4J and 4L, bacterial acquisition by BAIBA-injected ticks

218   was significantly reduced compared to the isomer-injected ticks (Fig. 4M). Collectively, our

219   findings indicated that D-BAIBA metabolism is important for *A. phagocytophilum* infection of

220   ticks.

221

222   **Disruption of D-BAIBA-related enzymes affects tick fitness.** Nucleotide metabolism

223   is important for physiological and cellular homeostasis[47]. Given our observations with *A.*

224   *phagocytophilum* colonization of ticks, we aimed to deconvolute the bacterial acquisition effect

225   of D-BAIBA metabolism from tick fitness. Therefore, we silenced nymphs for *upb1* or *agxt2*

226   (Figs. 5A and 5C) and measured attachment, feeding and survival. While we noticed a slight

227   impairment in attachment for *I. scapularis* microinjected with the *upb1* siRNA (fig. S18), reduced

228   weight in nymphs silenced for either *upb1* or *agxt2* was observed (Figs. 5B and 5D)*.

229   Interestingly, the feeding deficiency was also detected when nymphs were microinjected with

230   the *upb1* siRNA and fed on *A. phagocytophilum*-infected mice, but not in *agxt2*-silenced ticks

231   (fig. S19). Nymphs silenced for *upb1* or *agxt2* exhibited reduced survival post-feeding compared

232   to the control treatment (Figs. 5E-F). We then performed an experiment by microinjecting tick

233   nymphs with exogenous amounts of racemic BAIBA to evaluate whether this metabolite

234   influenced arthropod fitness. We used 16-80 pmols of racemic BAIBA in these experiments (fig.

235   S20A-B) because 40 pmols successfully phenocopied the *siagxt2* siRNA injection treatment

236   (Figs. 4K-M). There was no significant difference in attachment or weight for ticks injected with

237   the racemic BAIBA when compared to the control treatment (fig. S20C-D). Conversely, we

238   observed a dose-dependent decrease in survival for nymphs post-feeding (Fig. 5G).

239   Collectively, we determined that the enzymes involved in D-BAIBA metabolism affect tick

240   feeding and survival. These results indicated a pleiotropic role for the tick metabolite BAIBA in

241   tick fitness and bacterial acquisition.

Discussion

242

243   In this study, we sought to understand how resource allocation and metabolism influence

244   interspecies relationships. We developed a system for evaluating the metabolic status of tick

245   cells and demonstrated how bioenergetic disruption affects infection. We determined that the

246   ISE6 cell line is permissive to manipulation by small molecule inhibitors, which can be used for

247   measuring glycolysis and cellular respiration in tick cells. Using an adapted metabolic flux

248   assay, we observed that *A. phagocytophilum* and *B. burgdorferi* induce glycolysis but not

249   OxPhos in tick cells. This phenomenon was distinct from *R. buchneri* endosymbiosis,

250   suggesting a contrasting bacterial association in *I. scapularis*. In ticks, 2-DG and oligomycin

251   exhibit detrimental effects on attachment and molting, respectively. These observations offer

252   glimpses into the interconnection between bioenergetics and arthropod fitness, including how

253   metabolic arrest impacts organismal homeostasis. The bioenergetics platform described in this

254   study provides an invaluable tool for studying the metabolic interdependence between arthropod

255   vectors and their microbial partners, a topic that is regrettably understudied.

256   Treatment with OxPhos inhibitors promoted a striking increase of bacterial burden in tick

257   cells. Specifically, oligomycin, rotenone and antimycin A augmented *A. phagocytophilum* and *R.*

258   *buchneri* load in *I. scapularis* ISE6 cells. It is plausible that arresting OxPhos promotes a buildup

259   of substrates that rapidly accelerates bacterial division inside ticks. It is known that rickettsial

260   bacteria carry small genomes and require host nutrients for survival[48-50]. Using a metabolomics

261   approach, we compared changes that occur in tick cells infected with two obligate intracellular

262   bacteria: *A. phagocytophilum* and *R. buchneri*. We found that *A. phagocytophilum* was more

263   disruptive than the endosymbiont *R. buchneri*. It is possible that *A. phagocytophilum* draws

264   more intracellular resources than *R. buchneri*; or, alternatively, it requires additional pathways

265   for replication compared to *R. buchneri*. How ticks maintain cellular homeostasis when

266   metabolites are elevated is not fully understood. Likewise, it remains to be determined if

267   metabolite changes upon *A. phagocytophilum* infection are due to parasitism or a tick response

268   to the microbe.

269   Ticks are hosts of a variety of symbionts, including species belonging to the genera

270   *Coxiella, Rickettsia* and *Francisella*[31,51]. Symbionts are essential for arthropod development and

271   reproduction, as they provide essential vitamins and cofactors that ticks cannot sequester from

272   imbibed blood (*e.g.*, biotin and folate)[51,52]. *R. buchneri* encodes genes that may provide

273   essential vitamins and cofactors and can be detected at high prevalence in *I. scapularis*

274   populations[48,53], suggesting a possible selective advantage to the tick. This dependence

275   indicates that tick symbionts have evolved mechanisms to ensure a balance of energy storage

276   within the vector. This was noted in our metabolomics data, where we observed little to no

277   alterations in tick energy metabolism during *R. buchneri* infection. In contrast, the disruption of

278   tick metabolism by *A. phagocytophilum* is mirrored by its inability to be maintained transovarially

279   among *Ixodes* spp. populations. Whether tick metabolism contributes to transstadial or

280   transovarial transmission remains to be explored.

281   Given the metabolites uncovered in this study, we focused our efforts on hits that may

282   be representative of several pathways. We discovered that silencing genes involved in the

283   anabolism and catabolism of D-BAIBA reduced *A. phagocytophilum* burden and impaired tick

284   feeding and survival. These findings indicate that D-BAIBA may be acting within a defined

285   concentration window to enable tick fitness. We suggest that impairing D-BAIBA catabolism

286   through the injection of *agxt2* siRNA in *I. scapularis* may lead to a metabolite hyper-

287   accumulation and an alteration of the metabolic flux in ticks. On the other hand, altering D-

288   BAIBA anabolism via the injection of *upb1* siRNA in *I. scapularis* may generate a hypo-

289   accumulation of D-BAIBA. Decreased D-BAIBA levels in ticks likely inhibited downstream

290   biochemical networks and homeostasis in *I. scapularis*. Altogether, these findings highlight the

291   importance of a critical metabolite for life history programs in ticks, including maintenance,

292   growth and survival[17-20].

293   Finally, *A. phagocytophilum* altered metabolic pathways in ticks for efficient bacterial

294   acquisition. In mammals, BAIBA is involved in thermoregulation by promoting the browning of

295   adipose tissue[44]. Previous work demonstrated that *A. phagocytophilum* enhances tick survival

296   through cold tolerance[13]. Whether BAIBA confers a survival advantage or contributes to

297   thermoregulation of ticks remains unknown. Overall, we demonstrated that tools for studying

298   metabolic activity in mammals can be applied to arthropod vectors and their microbial

299   counterparts. Our findings highlight a shift in perspective for bioenergetics and resource

300   allocation when evaluating microbial associations in arthropod vectors.

Materials and Methods

Cell culture

301

302

303 The *I. scapularis* IDE12 and ISE6, *A. americanum* AAE2 and *D. andersoni* DAE100 cell

304 lines were obtained from Dr. Ulrike Munderloh at the University of Minnesota. All tick cell lines

305 were maintained at 34°C in a non-CO$_2$ incubator. Cells were cultured in T25 cm flasks (Greiner

306 bio-one) containing L15C300 medium supplemented with 10% heat-inactivated fetal bovine

307 serum (FBS, Millipore-Sigma), 10% tryptose phosphate broth (TPB, Difco), 0.1% bovine

308 cholesterol lipoprotein concentrate (LPPC, MP Biomedicals). For *in vitro* experiments, ISE6 cells

309 were plated in 48-well plates at a density of $1X10^6$ cells per well. The human leukemia cell line

310 HL-60 was obtained from ATCC and maintained at 37°C in a 5% CO$_2$ containing incubator.

311 Cells were cultured in T25 vented flasks (Cyto One) containing RPMI-1640 medium with L-

312 Glutamine (Quality Biological) supplemented with 10% FBS (Gemini Bio-Products) and 1%

313 GlutaMax (Gibco). All cell cultures were tested for *Mycoplasma* (Southern Biotech).

314

Bacteria, mice and ticks

315

316 *A. phagocytophilum* strain HZ was grown as previously described in HL-60 cells at 37°C,

317 using RPMI medium supplemented with 10% Fetal Bovine Serum and 1% Glutamax[54]. Bacterial

318 numbers were calculated using the formula: number of infected HL-60 cells × 5 morulae/cell ×

319 19 bacteria/cell × 0.5 (representing 50% recovery rate)[55]. Bacteria were purified by passing

320 infected cells through a 27-gauge bent needle and using a series of centrifugation steps, as

321 previously described[54]. Low passage isolate of *B. burgdorferi* B31 clone MSK5 was cultured in

322 Barbour-Stoenner Kelly (BSK)-II medium supplemented with 6% normal rabbit serum at 34°C[56],

323 never exceeding 10^8 bacteria per ml. Plasmid profiling was performed as described elsewhere[56].

324 *R. buchneri* strain ISO7^T was obtained from Dr. Ulrike Munderloh. *R. buchneri* was maintained in

325 ISE6 cells at 30°C in a non-CO$_2$ incubator[6]. Bacteria were isolated from infected ISE6 cells

326 using a 27-gauge needle and cell debris was separated by centrifugation at 600xg for 10 mins.

327   Spirochetes were counted using a light- or dark-field (Zeiss Primo Star Microscope) under a 40X

328   objective lens, respectively[56].

329   Age matched, six- to ten-week-old C57BL/6J male mice were supplied by the University

330   of Maryland Veterinary Resources or Jackson Laboratories. *I. scapularis* nymphs were obtained

331   from either Oklahoma State University or the University of Minnesota breeding colonies. Upon

332   arrival, ticks were housed in an incubator at 23°C with >85% relative humidity and a 14/10-hour

333   light/dark photoperiod regimen. Animal experiments were approved by the Institutional Biosafety

334   (IBC, IBC-00002247) and Animal Care and Use (IACUC, #0119012) committees at the

335   University of Maryland School of Medicine and complied with National Institutes of Health (NIH)

336   guidelines (Office of Laboratory Animal Welfare [OLAW] assurance number A3200-01).

337

338   **RNA interference and tick injection experiments**

339   Small interfering RNAs (siRNA) and their scrambled controls (scRNA) were synthesized

340   using the Silencer siRNA construction kit (Thermo Scientific) according to the manufacturer's

341   instructions. Nymphs were microinjected with 30-50 ng of siRNA or scRNA, as previously

342   described[57]. Ticks were allowed to recover overnight before being placed on uninfected or *A.*

343   *phagocytophilum*-infected C57BL/6J mice. Ticks were collected 3 days after placement in which

344   the degree of host attachment and tick weight were assessed. Ticks were either placed in a

345   incubator (23°C, with >85% relative humidity in a 14/10-hour light/dark photoperiod regimen) for

346   survival experiments lasting 18 days or frozen at -80°C in 200 ml TRIzol reagent for RNA

347   extraction.

348   For BAIBA and inhibitor treatments, ticks were microinjected with 60-80 nl of BAIBA or

349   inhibitor solution and allowed to recover overnight. The following day, ticks were placed on

350   anesthetized mice. Three days after placement, tick attachment and weight were recorded, and

351   collected ticks were either placed in a humidified chamber for survival/molting experiments or

352   frozen in TRIzol reagent for RNA extraction. For molting experiments, *I. scapularis* were

353   monitored until ticks in the control treatment molted.

354

355   **Mouse infections**

356   Age matched, six- to ten-week-old C57BL/6J male mice were used for *A.*

357   *phagocytophilum* acquisition experiments. *A. phagocytophilum* was isolated from infected HL-60

358   cells and resuspended in PBS at a concentration of 1×10^8 bacteria per ml. Mice were

359   intraperitoneally injected with 100 µl of the inoculum (1×10^7 total *A. phagocytophilum*). Infection

360   progressed for 7 days before placing ticks.

361

362   **Bioenergetic measurements in ISE6 cells using the Seahorse analyzer**

363   OCR and ECAR were measured in XF96 cell culture microplates using a Seahorse

364   XFe96 Extracellular Flux Analyzer (Seahorse, Agilent Technologies). ISE6 cells were seeded at

365   densities of 120 – 150,000 cells per well in complete L15C300 media[41] and incubated at 34°C

366   for 24 hours. Media was then replaced with modified L15C media (mL15C) alone or mL15C

367   containing *A. phagocytophilum*, *B. burgdorferi* or *R. buchneri* for 48 hours (table S1). For OCR

368   detection, values were measured at basal conditions and after 20 µM 2,4-DNP (Sigma Aldrich),

369   0.1 µM rotenone (Sigma Aldrich) and 0.5 µM antimycin A (Sigma Aldrich) treatments. For ECAR

370   detection, values were measured at basal conditions and after adding 50 mM glucose and 2-DG

371   (Sigma Aldrich). Data normalization was performed using a Celigo image cytometer (Nexcelom

372   Bioscience, Massachusetts) following the manufacturer guidelines for measuring cell

373   confluency. The cartridge was calibrated with the Seahorse XF Calibrant Solution (Agilent

374   Technologies) at 37°C in a non-CO_2 and non-humidified incubator for at least 2 h prior to the

375   assay.

376

377   **qRT-PCR analysis**

17

378   Tick and cell samples were preserved in the TRIzol reagent prior to RNA extraction.

379   Total RNA was isolated using the PureLink RNA Mini kit (Ambion). cDNA was synthesized from

380   300-600 ng RNA using the Verso cDNA Synthesis kit (ThermoFisher). Gene expression was

381   measured using a CFX96 Touch Real-Time PCR Detection System (Bio-rad) with iTaq

382   Universal SYBR Green Supermix (Bio-rad). Expression levels for genes were calculated by

383   relative quantification normalized to tick *actin*. Primers used are listed in table S2.

384

Metabolomics

386   To generate samples for metabolomics, 5×10^7 ISE6 cells were placed in T25 flasks in

387   L15C300 media. The following day, media was removed and replaced with mL15C media alone

388   or mL15C media containing either *A. phagocytophilum* or *R. buchneri* at a MOI 50. Cells were

389   harvested via a cell scraper at 1 hour and 24 hours post-infection followed by centrifugation at

390   3,320xg for 10 minutes at 4°C. Cell pellets were frozen in liquid nitrogen and shipped to

391   Metabolon Inc. for analysis. Four independent experiments were performed for each condition,

392   and data were normalized according to protein concentrations.

393   Sample processing was performed at Metabolon Inc., as previously described[58].

394   Individual samples were subjected to methanol extraction and then separated into aliquots for

395   ultra-high performance liquid chromatography/mass spectrometry (UHPLC/MS). Global

396   biochemical profiling involved reverse phase chromatography positive ionization for hydrophilic

397   (LC/MS Positive Polar) and hydrophobic (LC/MS Positive Lipid) compounds, reverse phase

398   chromatography with negative ionization (LC/MS Negative), and a hydrophilic interaction

399   chromatography (HILIC) coupled to negative ion mode electrospray ionization (LC/MS Polar)[59].

400   Methods interspersed between full mass spectrometry and refragmentation (MSn) scans.

401   Metabolites were identified by automated comparison of the ion features in the experimental

402   samples to a reference library of at least 4000 chemical standard entries[60].

403   Metabolon Inc. performed the initial statistical analysis for the metabolite study. Two

404   types of statistical analyses were performed: (1) significance tests and (2) classification

405   analysis. Standard statistical analyses were performed in ArrayStudio on log-transformed data.

406   For non-standard analyses RStudio was used. Following log transformation, Welch's two

407   sample t-test identified biochemicals that differed significantly ($p < 0.05$) and false discovery rate

408   (q value) were calculated between treatments. Principal components analysis, hierarchical

409   clustering, and random forest were used for metabolite classification. Time points were equaled

410   to 1 and each compound in the original scale (raw area count) was rescaled to set the median

411   across samples. Data are available via MetaboLights, identifier MTBLS686.

412

413   **Colorimetric assays**

414   ISE6 cells were seeded in 48-well microtiter plate (Cyto-one) with complete L15C300

415   medium at a density of $1x10^6$ for 24 hours. Cells were challenged with *A. phagocytophilum*, *B.*

416   *burgdorferi* or *R. buchneri* (MOI 50) in mL15C media supplemented with 10 mM glucose and

417   incubated for 1 or 24 hours. Cells were harvested and resuspended in assay buffer. Glycolytic

418   activity was evaluated using kits measuring lactate (Sigma Aldrich), lactate dehydrogenase

419   (LDH, Sigma Aldrich), phosphoglucose isomerase (PGI, Sigma Aldrich) and nicotinamide

420   adenine dinucleotide (NAD/NADH, Sigma Aldrich). TCA cycle activity was evaluated from kits

421   measuring citrate (Sigma Aldrich), aconitase activity (Sigma Aldrich), succinate (Sigma Aldrich)

422   and succinate dehydrogenase activity (SDH, Sigma Aldrich). Reagents are listed in table S3.

423

424   **Statistical analysis**

425   Statistical significance between two conditions were assessed using an unpaired t-test

426   with Welch's correction for unequal variances. One-way ANOVA followed by the Dunnett's

427   multiple comparisons test was used for analyzing statistical differences between three or more

428   groups. For categorical variables, Fisher's Exact or Chi-square test was used. Survival curves

19

429   were analyzed with the Log-rank (Mantel-Cox) test. All statistical analysis were performed in

430   GraphPad PRISM® (GraphPad Software version 9.1.0). Outliers were detected by a Graphpad

431   Quickcals program (https://www.graphpad.com/quickcalcs/Grubbs1.cfm).

Figure Legends

Figure 1: Glycolysis and OxPhos are critical metabolic pathways for fitness programs in

I. scapularis. **A.** Abbreviated representation of glycolysis (green), TCA (pink) and OxPhos

(blue) with inhibitors that block enzymatic function (red). (**B-F**). Viability measurement of 1x 10^6

ISE6 cells. Cells were treated with the corresponding inhibitors at indicated concentrations for

48 hours prior to analysis. Data are representative of at least two independent experiments

N=4-8. Concentrations that caused a significant decrease in viability are shaded red and non-

significant effects are highlighted in blue. **G.** Extracellular acidification rate (ECAR) of 1.2x 10^5

ISE6 cells treated with chemical inhibitors. Glucose (Glu) and 2-Deoxy-D-Glucose

(2-DG) were administered at 25 mM and 50 mM, respectively. Data are representative of at

least three independent experiments N=6. **H.** Oxygen consumption rate (OCR) of 1.2x 10^5 ISE6

cells treated with chemical inhibitors. 2,4-Dinitrophenol (DNP), rotenone and antimycin were

administered at 20 µM, 0.1 µM and 0.5 µM, respectively. Data are representative of at least two

independent experiments N=6. **I.** Ticks were injected with the respective amounts of 2-DG and

placed on C57BL/6 mice overnight (grey). Percentage of ticks that successfully attached on

C57BL/6 mice are displayed in blue. Data are representative of at least two independent

experiments. Number of ticks used ranged from 25-100 per treatment. **J.** Molting length of ticks

following microinjection with oligomycin. Ticks were injected with a sublethal amount of

oligomycin (0.8 pmol) prior to feeding. **K.** Percentage of ticks that molted following feeding.

Number of ticks used in **J** and **K** ranged from 10-11 per treatment. (**B-F**) One-way ANOVA

followed by Dunnett's test. (**I**) Chi-square test. (**J**) Log rank (Mantel-Cox) test. (**K**) Fisher's exact

test. *, $p<0.05$. Anti = Antimycin A, Rot=rotenone. NS – not significant.

Figure 2: *A. phagocytophilum* and *B. burgdorferi* induce glycolysis upon infection of tick

cells. A. Schematics of infection assay. *I. scapularis* ISE6 cells were cultured in L15C300

medium. At day 0, the L15C300 medium was replaced with the mL15C medium for cell culture.

21

458   Tick cells were infected with distinct microbial agents at indicated MOI and the Seahorse

459   analysis was done at day 2 post-infection. **B-D.** Extracellular acidification rate (ECAR) of 1.2

460   x10^5 ISE6 cells stimulated with (**B**) *A. phagocytophilum*, (**C**) *B. burgdorferi*, or (**D**) *R. buchneri*.

461   Data normalized to unstimulated cells. Data are representative of three independent

462   experiments N=6. **E-G.** Oxygen consumption rate (OCR) of 1.2 x10^5 ISE6 cells stimulated with

463   (**E**) *A. phagocytophilum*, (**F**) *B. burgdorferi*, or (**G**) *R. buchneri*. Data normalized to unstimulated

464   cells. Data are representative of at least three independent experiments N=6. MOI=multiplicity

465   of infection. Glu=Glucose, 2-DG=2-deoxy-glucose, DNP=2,4-dinitrophenol, Rot=rotenone,

466   Anti=antimycin. DNP, Rot and Anti were administered at 20 µM, 0.1 µM and 0.5 µM,

467   respectively. Glu and 2-DG were administered at 25 mM and 50 mM, respectively.

468

469   **Figure 3: *A. phagocytophilum* and *B. burgdorferi* enhance the glycolytic flux from**

470   **glucose to lactate in tick cells. A.** Schematic representation of glycolysis (green), TCA (pink)

471   and OxPhos (blue). Readouts for the glycolytic flux to lactate in tick ISE6 cells are highlighted in

472   red. (**B-M**) 1 x10^6 ISE6 cells were stimulated with *A. phagocytophilum* at a multiplicity of

473   infection (MOI 50) (blue), *B. burgdorferi* (MOI 50) (red), *R. buchneri* (MOI 50) (orange) or left

474   unstimulated (grey) for 1 or 24 hours. (**B-D**) Phosphoglucoisomerase (PGI) and (**E-G**) lactate

475   dehydrogenase (LDH) activity, (**H-J**) lactate and (**K-M**) nicotinamide adenine

476   dinucleotide (NADH) measurements through colorimetric assays. Data represent at least two

477   independent experiments N=5. Statistical significance was evaluated by the unpaired t test with

478   Welch's correction. *, *p*<0.05. NS – not significant.

479

480   **Figure 4: *A. phagocytophilum* depends on tick cell metabolites for *I. scapularis* infection.**

481   **A.** Schematics of microbial infection upon inhibitor treatment. **B-C** 1 x10^6 ISE6 cells were

482   treated with oligomycin – 0.5 µM; 2,4-DNP - 20 µM; rotenone – 0.1 µM; antimycin A – 0.5 µM or

483   2-DG – 50 mM 1 hour prior to infection. Cells were then incubated with (**B**) *A. phagocytophilum*

484   (MOI 50) or (**C**) *R. buchneri* (MOI 50) for 48 hours. Data were normalized to untreated but

485   infected control cells (-) to calculate fold changes in bacterial load. Data are representative of at

486   least three independent experiments N=4-6. **D.** Schematics of BAIBA metabolism. Enzymes

487   involved in catabolism and anabolism of BAIBA are highlighted in red. **E.** BAIBA levels

488   measured in uninfected, *A. phagocytophilum*-infected, or *R. buchneri*-infected 5 x10^7 ISE6 cells

489   at MOI 50 24 hours post-infection N=4-6. **F-H.** Gene expression of ticks fed on uninfected mice

490   or mice infected with *A. phagocytophilum*. Relative expression of (**F**) *upb1*, (**G**) *agxt2*, or (**H**)

491   *abat* normalized to tick *actin*. Data are representative of two independent experiments N=10. **I-**

492   **L.** Nymphs were injected with siRNA or scrambled control before feeding on *A.*

493   *phagocytophilum*-infected mice for three days. Silencing efficiency in (**I**) *upb1* or (**K**) *agxt2* ticks.

494   (**J** and **L**) *A. phagocytophilum* burden in silenced and control ticks. Bacterial burden was

495   calculated by using the *A. phagocytophilum* specific *16S* rDNA gene and its relative expression

496   normalized to *actin*. Data are representative of at least three independent experiments N=22-33.

497   **M.** *A. phagocytophilum* burden in BAIBA-treated ticks. Nymphs were injected with 40 pmol of

498   BAIBA, the α-aminoisobutyric acid (isomer) or phosphate-buffered saline (PBS) (-) and ticks

499   were placed on *A. phagocytophilum*-infected mice for three days. Bacterial burden was

500   calculated by using the *A. phagocytophilum* specific *16S* rDNA gene and its relative expression

501   normalized to *actin*. Data are representative of two independent experiments N=24-28.

502   Statistical significance was evaluated by one-way ANOVA followed by Dunnett's post-hoc test

503   (**B**, **C**, **E** and **M**) or unpaired t test with Welch's correction (**F-L**). *, $p<0.05$. NS=not significant.

504

505   **Figure 5: BAIBA regulates tick feeding and survival. A.** Silencing efficiency of *upb1* in ticks.

506   Nymphs were injected with the *upb1* siRNA (*siupb1*) or scrambled control (*scupb1*) before ticks

507   were placed on uninfected mice to feed for three days. N=21-26. **B.** Weight of ticks post-feeding

508   N=21-26. **C.** Silencing efficiency of *agxt2* in ticks. Nymphs were injected with the *agxt2* siRNA

509   (*siagxt2*) or scrambled control sequence (*scagxt2*) before ticks were placed on uninfected mice

510   to feed for three days. N=16-20. **D.** Weight of ticks post-feeding N=16-20. **E.** Survival of *siupb1-*

511   or *scupb1*-injected ticks recorded 18 days post-blood meal N=23-26. **F.** Survival of *siagxt2-* or

512   *scagxt2*-injected ticks recorded 18 days post-blood meal. N=17-19. Data are representative of

513   at two independent experiments. **G.** Nymphs were injected with corresponding amounts of

514   BAIBA before feeding on mice. Survival was recorded for 18 days. Data are representative of

515   two independent experiments N=9-14. Statistical significance was evaluated by (**A-D**) unpaired t

516   test with Welch's correction or (**E-G**) Log rank (Mantel-Cox) test. *, $p<0.05$. NS=not significant.

533 **Author contributions**

534   SS and JHFP designed the study. SS, AR, LM, AJO, NS, XW, HJL, LRB, FECP and PR

535 performed the experiments. SS, AJO, HJL, and JHFP wrote the manuscript. LRB aided with

536 experimentation and created some schematics. All authors analyzed the data, provided

537 intellectual input into the study, and contributed to editing of the manuscript. GMF and BMP

538 supervised experiments and provided instruments. JHFP supervised the study.

539

References

540

541   1   WHO. Vector-borne diseases, <https://www.who.int/news-room/fact-sheets/detail/vector-

542   borne-diseases> (2020).

543   2   Kurokawa, C. *et al.* Interactions between *Borrelia burgdorferi* and ticks. *Nat Rev*

544   *Microbiol* **18**, 587-600 (2020). https://doi.org:10.1038/s41579-020-0400-5

545   3   Lochhead, R. B., Strle, K., Arvikar, S. L., Weis, J. J. & Steere, A. C. Lyme arthritis:

546   linking infection, inflammation and autoimmunity. *Nature Reviews Rheumatology* **17**,

547   449-461 (2021). https://doi.org:10.1038/s41584-021-00648-5

548   4   O'Neal, A. J., Singh, N., Mendes, M. T. & Pedra, J. H. F. The genus *Anaplasma*: drawing

549   back the curtain on tick-pathogen interactions. *Pathogens and Disease* **79**, ftab022

550   (2021). https://doi.org:10.1093/femspd/ftab022

551   5   Smith, R. P. Tick-borne diseases of humans. *Emerg Infect Dis* **11**, 1808-1809 (2005).

552   https://doi.org:10.3201/eid1111.051160

553   6   Kurtti, T. J. *et al. Rickettsia buchneri* sp. nov., a rickettsial endosymbiont of the

554   blacklegged tick *Ixodes scapularis. International Journal of Systematic and Evolutionary*

555   *Microbiology* **65**, 965 (2015).

556   7   Verhoeve, V. I., Fauntleroy, T. D., Risteen, R. G., Driscoll, T. P. & Gillespie, J. J. Cryptic

557   genes for interbacterial antagonism distinguish *Rickettsia* species infecting blacklegged

558   ticks from other *Rickettsia* pathogens. *Frontiers in Cellular and Infection Microbiology* **12**,

559   880813 (2022). https://doi.org:10.3389/fcimb.2022.880813

560   8   Hagen, R., Verhoeve, V. I., Gillespie, J. J. & Driscoll, T. P. Conjugative transposons and

561   their cargo genes vary across natural populations of *Rickettsia buchneri* infecting the tick

562   *Ixodes scapularis. Genome Biology and Evolution* **10**, 3218-3229 (2018).

563   https://doi.org:10.1093/gbe/evy247

564   9   Sidak-Loftis, L. C. *et al.* The unfolded-protein response triggers the arthropod Immune

565   Deficiency pathway. *mBio* **13**, e0070322 (2022). https://doi.org:10.1128/mbio.00703-22

566   10   Cabezas-Cruz, A., Espinosa, P., Alberdi, P. & de la Fuente, J. Tick-pathogen

567   interactions: the metabolic perspective. *Trends in Parasitology* **35**, 316-328 (2019).

568   https://doi.org:10.1016/j.pt.2019.01.006

569   11   Samaddar, S., Marnin, L., Butler, L. R. & Pedra, J. H. F. Immunometabolism in arthropod

570   vectors: redefining interspecies relationships. *Trends in Parasitology* **36**, 807–815.

571   (2020). https://doi.org:10.1016/j.pt.2020.07.010

572   12   Shaw, D. K. *et al.* Vector immunity and evolutionary ecology: the harmonious

573   dissonance. *Trends in Immunology* **39**, 862–873. (2018).

574   https://doi.org:10.1016/j.it.2018.09.003

575   13   Neelakanta, G., Sultana, H., Fish, D., Anderson, J. F. & Fikrig, E. *Anaplasma*

576   *phagocytophilum* induces *Ixodes scapularis* ticks to express an antifreeze glycoprotein

577   gene that enhances their survival in the cold. *The Journal of Clinical Investigation* **120**,

578   3179-3190 (2010). https://doi.org:10.1172/JCI42868

579   14   Duron, O. *et al.* Tick-bacteria mutualism depends on B vitamin synthesis pathways.

580   *Current Biology* **28**, 1896-1902 e1895 (2018). https://doi.org:10.1016/j.cub.2018.04.038

581   15   Zhong, Z. *et al.* Symbiont-regulated serotonin biosynthesis modulates tick feeding

582   activity. *Cell Host & Microbe* **29**, 1545-1557 e1544 (2021).

583   https://doi.org:10.1016/j.chom.2021.08.011

584   16   Perrin, N., Christe, P. & Richner, H. On host life-history response to parasitism. *Oikos*

585   **75**, 317-320 (1996). https://doi.org:10.2307/3546256

586   17   Stearns, S. C., Rose, M. R. & Mueller, L. D. The evolution of life histories. . *Journal of*

587   *Evolutionary Biology* **6**, 304-306 (1992). https://doi.org:https://doi.org/10.1046/j.1420-

588   9101.1993.6020304.x

589   18   Boggs, C. Resource allocation: exploring connections between foraging and life history.

590   *Functional Ecology* **6**, 508-518 (1992).

591   19   Roff, D. *Evolution of life histories: theory and analysis*. (Springer Science & Business

592   Media, 1993).

593   20   Burger, J. R., Hou, C. & Brown, J. H. Toward a metabolic theory of life history.

594   *Proceedings of the National Academy of Sciences of the United States of America* **116**,

595   26653-26661 (2019). https://doi.org:10.1073/pnas.1907702116

596   21   Wang, A., Luan, H. H. & Medzhitov, R. An evolutionary perspective on

597   immunometabolism. *Science* **363**, eaar3932 (2019).

598   https://doi.org:10.1126/science.aar3932

599   22   Russell, D. G., Huang, L. & VanderVen, B. C. Immunometabolism at the interface

600   between macrophages and pathogens. *Nat Rev Immunol* **19**, 291-304 (2019).

601   https://doi.org:10.1038/s41577-019-0124-9

602   23   Warburg, O., Posener, K. & Negelein, E. Über den stoffwechsel der carcinomzelle.

603   *Naturwissenschaften* **12**, 1131-1137 (1924).

604   24   Ward, P. S. & Thompson, C. B. Metabolic reprogramming: a cancer hallmark even

605   warburg did not anticipate. *Cancer Cell* **21**, 297-308 (2012).

606   25   DeBerardinis, R. J., Lum, J. J., Hatzivassiliou, G. & Thompson, C. B. The biology of

607   cancer: metabolic reprogramming fuels cell growth and proliferation. *Cell Metabolism* **7**,

608   11-20 (2008).

609   26   Hall, S. R., Simonis, J. L., Nisbet, R. M., Tessier, A. J. & Cáceres, C. E. Resource

610   ecology of virulence in a planktonic host-parasite system: an explanation using dynamic

611   energy budgets. *The American Naturalist* **174**, 149-162 (2009).

612   27   Peyraud, R., Cottret, L., Marmiesse, L., Gouzy, J. & Genin, S. A resource allocation

613   trade-off between virulence and proliferation drives metabolic versatility in the plant

614   pathogen *Ralstonia solanacearum*. *PLoS Pathogens* **12**, e1005939 (2016).

615   28   Hite, J. L., Pfenning, A. C. & Cressler, C. E. Starving the enemy? Feeding behavior

616   shapes host-parasite interactions. *Trends in Ecology & Evolution* **35**, 68-80 (2020).

617   29   Cressler, C. E., Nelson, W. A., Day, T. & McCauley, E. Disentangling the interaction

618   among host resources, the immune system and pathogens. *Ecol Lett* **17**, 284-293

619   (2014). https://doi.org:10.1111/ele.12229

620   30   Voss, K. *et al.* A guide to interrogating immunometabolism. *Nat Rev Immunol* **21**, 637-

621   652 (2021). https://doi.org:10.1038/s41577-021-00529-8

622   31   Song, X., Zhong, Z., Gao, L., Weiss, B. L. & Wang, J. Metabolic interactions between

623   disease-transmitting vectors and their microbiota. *Trends in Parasitology* **38**, 697-708

624   (2022). https://doi.org:10.1016/j.pt.2022.05.002

625   32   Villar, M. *et al.* Integrated metabolomics, transcriptomics and proteomics identifies

626   metabolic pathways affected by *Anaplasma phagocytophilum* infection in tick cells.

627   *Molecular & Cellular Proteomics* **14.12**, 3154-3172 (2015). https://doi.org:10.1074/mcp

628   33   Hoxmeier, J. C. *et al.* Metabolomics of the tick-*Borrelia* interaction during the nymphal

629   tick blood meal. *Scientific Reports* **7**, 1-11 (2017). https://doi.org:10.1038/srep44394

630   34   Cabezas-Cruz, A., Alberdi, P., Valdes, J. J., Villar, M. & de la Fuente, J. *Anaplasma*

631   *phagocytophilum* infection subverts carbohydrate metabolic pathways in the tick vector,

632   *Ixodes scapularis*. *Front Cell Infect Microbiol* **7**, 23 (2017).

633   https://doi.org:10.3389/fcimb.2017.00023

634   35   Alberdi, P. *et al.* The redox metabolic pathways function to limit *Anaplasma*

635   *phagocytophilum* infection and multiplication while preserving fitness in tick vector cells.

636   *Sci Rep* **9**, 13236 (2019). https://doi.org:10.1038/s41598-019-49766-x

637   36   Dahmani, M., Anderson, J. F., Sultana, H. & Neelakanta, G. Rickettsial pathogen uses

638   arthropod tryptophan pathway metabolites to evade reactive oxygen species in tick cells.

639   *Cellular Microbiology* **22**, e13237 (2020). https://doi.org:10.1111/cmi.13237

640   37   Namjoshi, P., Dahmani, M., Sultana, H. & Neelakanta, G. Rickettsial pathogen inhibits

641   tick cell death through tryptophan metabolite mediated activation of p38 MAP kinase.

642   *iScience* **26**, 105730 (2023). https://doi.org:10.1016/j.isci.2022.105730

38   Ramasamy, E., Taank, V., Anderson, J. F., Sultana, H. & Neelakanta, G. Repression of tick microRNA-133 induces organic anion transporting polypeptide expression critical for *Anaplasma phagocytophilum* survival in the vector and transmission to the vertebrate host. *PLoS Genetics* **16**, e1008856 (2020). https://doi.org:10.1371/journal.pgen.1008856

39   Mookerjee, S. A., Gerencser, A. A., Nicholls, D. G. & Brand, M. D. Quantifying intracellular rates of glycolytic and oxidative ATP production and consumption using extracellular flux measurements. *J Biol Chem* **292**, 7189-7207 (2017). https://doi.org:10.1074/jbc.M116.774471

40   Nicholls, D. G. *et al.* Bioenergetic profile experiment using C2C12 myoblast cells. *J Vis Exp* (2010). https://doi.org:10.3791/2511

41   Munderloh, U. G., Liu, Y., Wang, M., Chen, C. & Kurtti, T. J. Establishment, maintenance and description of cell lines from the tick *Ixodes scapularis*. *The Journal of Parasitology* **80**, 533-543 (1994).

42   Troha, K. & Ayres, J. S. Metabolic adaptations to infections at the organismal level. *Trends in Immunology* **41**, 113-125 (2020). https://doi.org:https://doi.org/10.1016/j.it.2019.12.001

43   Rosenberg, G., Riquelme, S., Prince, A. & Avraham, R. Immunometabolic crosstalk during bacterial infection. *Nat Microbiol* **7**, 497-507 (2022). https://doi.org:10.1038/s41564-022-01080-5

44   Roberts, L. D. *et al.* β-Aminoisobutyric acid induces browning of white fat and hepatic β-oxidation and is inversely correlated with cardiometabolic risk factors. *Cell Metab* **19**, 96-108 (2014). https://doi.org:10.1016/j.cmet.2013.12.003

45   Tanianskii, D. A., Jarzebska, N., Birkenfeld, A. L., O'Sullivan, J. F. & Rodionov, R. N. β-aminoisobutyric acid as a novel regulator of carbohydrate and lipid metabolism. *Nutrients* **11** (2019). https://doi.org:10.3390/nu11030524

668 46   Sharma, A. *et al.* Cas9-mediated gene editing in the black-legged tick, *Ixodes scapularis*,

669   by embryo injection and ReMOT Control. *iScience* **25**, 103781 (2022).

670   https://doi.org:10.1016/j.isci.2022.103781

671 47   Lane, A. N. & Fan, T. W. Regulation of mammalian nucleotide metabolism and

672   biosynthesis. *Nucleic Acids Res* **43**, 2466-2485 (2015).

673   https://doi.org:10.1093/nar/gkv047

674 48   Driscoll, T. P. *et al.* Wholly *Rickettsia*! reconstructed metabolic profile of the

675   quintessential bacterial parasite of eukaryotic cells. *mBio* **8,** e00859-17 (2017).

676   https://doi.org:10.1128/mBio.00859-17

677 49   McClure, E. E. *et al.* Engineering of obligate intracellular bacteria: progress, challenges

678   and paradigms. *Nature Reviews Microbiology* **15**, 544-558 (2017).

679   https://doi.org:10.1038/nrmicro.2017.59

680 50   Salje, J. Cells within cells: Rickettsiales and the obligate intracellular bacterial lifestyle.

681   *Nature Reviews Microbiology* **19**, 375-390 (2021). https://doi.org:10.1038/s41579-020-

682   00507-2

683 51   Narasimhan, S. *et al.* Grappling with the tick microbiome. *Trends in Parasitology* **37**,

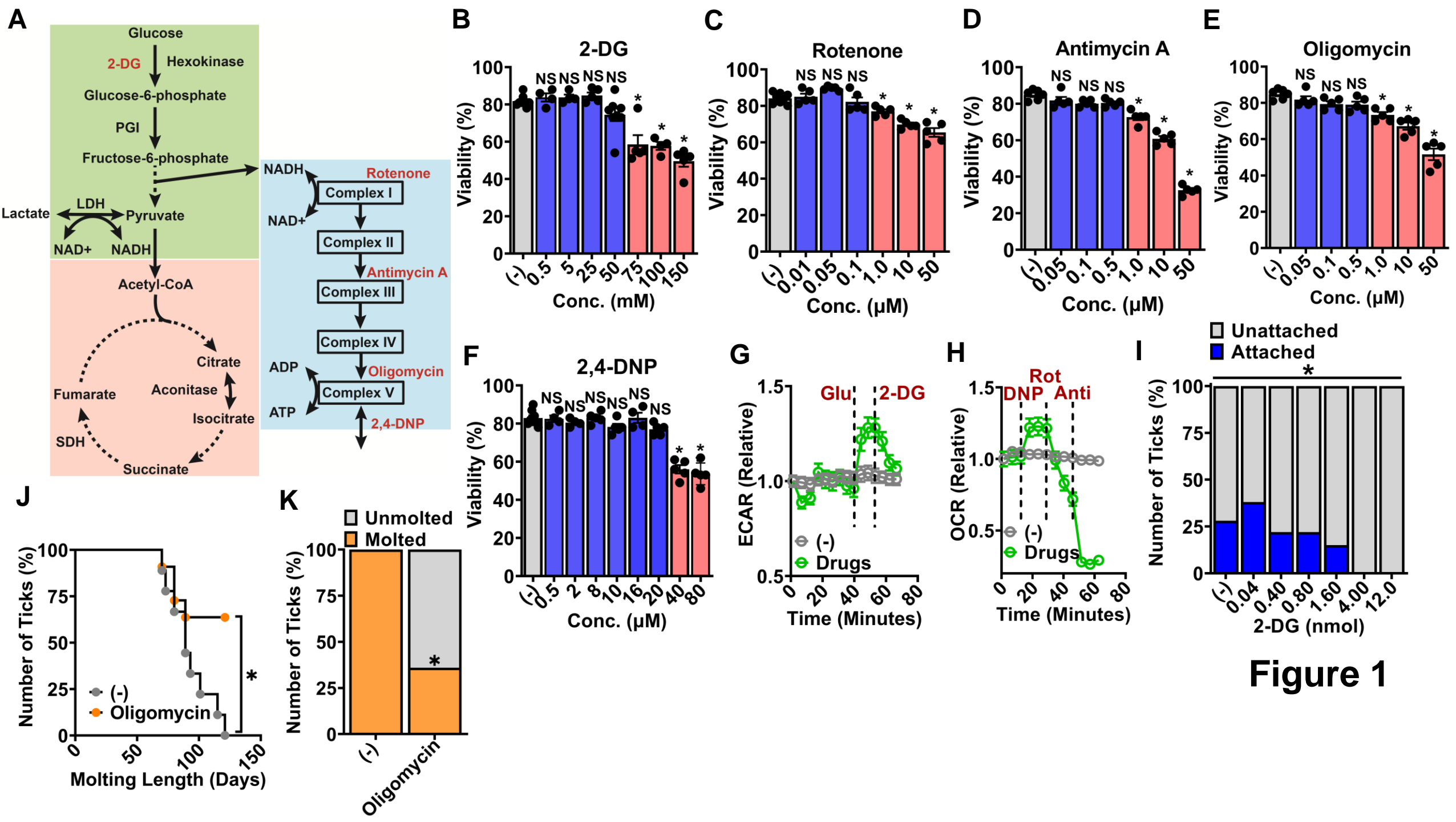684   722-733 (2021). https://doi.org:10.1016/j.pt.2021.04.004

685 52   Buysse, M. *et al.* A dual endosymbiosis supports nutritional adaptation to hematophagy

686   in the invasive tick *Hyalomma marginatum*. *Elife* **10** (2021).

687   https://doi.org:10.7554/eLife.72747

688 53   Oliver, J. D. *et al.* Growth dynamics and antibiotic elimination of symbiotic *Rickettsia*

689   *buchneri* in the tick *Ixodes scapularis* (Acari: Ixodidae). *Appl Environ Microbiol* **87** (2021).

690   https://doi.org:10.1128/AEM.01672-20
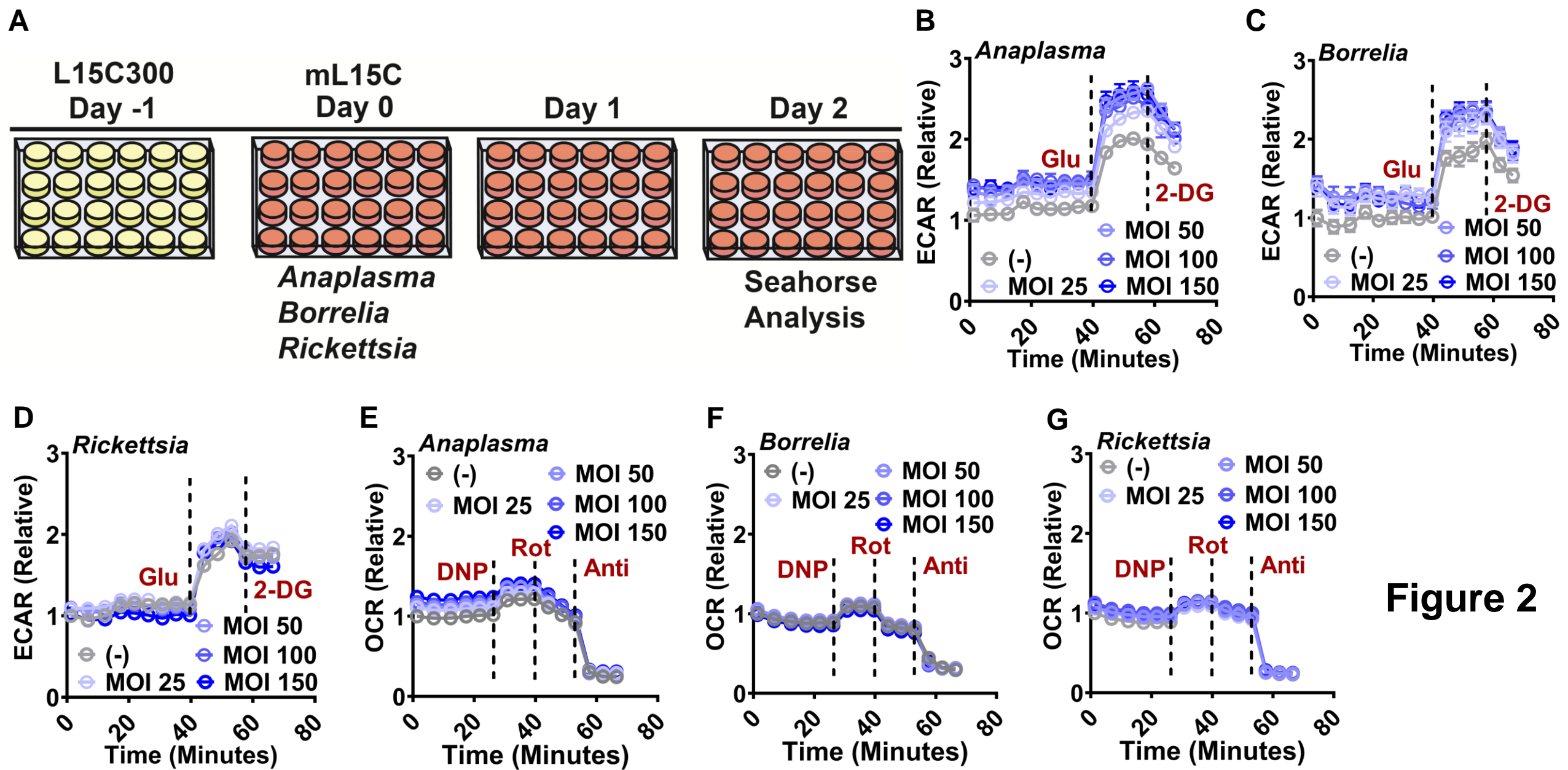
691 54   Oliva Chávez, A. S. *et al.* Tick extracellular vesicles enable arthropod feeding and

692   promote distinct outcomes of bacterial infection. *Nature Communications* **12**, 3696

693   (2021). https://doi.org:10.1038/s41467-021-23900-8

694   55   Yoshiie, K., Kim, H. Y., Mott, J. & Rikihisa, Y. Intracellular infection by the human

695   granulocytic ehrlichiosis agent inhibits human neutrophil apoptosis. *Infection and*

696   *Immunity* **68**, 1125-1133 (2000).

697   56   Labandeira-Rey, M. & Skare, J. T. Decreased infectivity in *Borrelia burgdorferi* strain

698   B31 is associated with loss of linear plasmid 25 or 28-1. *Infection and Immunity* **69**, 446-

699   455 (2001).

700   57   Shaw, D. K. *et al.* Infection-derived lipids elicit an immune deficiency circuit in

701   arthropods. *Nature communications* **8**, 14401 (2017).

702   58   Collet, T.-H. *et al.* A metabolomic signature of acute caloric restriction. *The Journal of*

703   *Clinical Endocrinology & Metabolism* **102**, 4486-4495 (2017).

704   59   Evans, A. *et al.* High resolution mass spectrometry improves data quantity and quality as

705   compared to unit mass resolution mass spectrometry in high-throughput profiling

706   metabolomics. *Metabolomics* **4**, 1 (2014).

707   60   DeHaven, C. D., Evans, A. M., Dai, H. & Lawton, K. A. Organization of GC/MS and

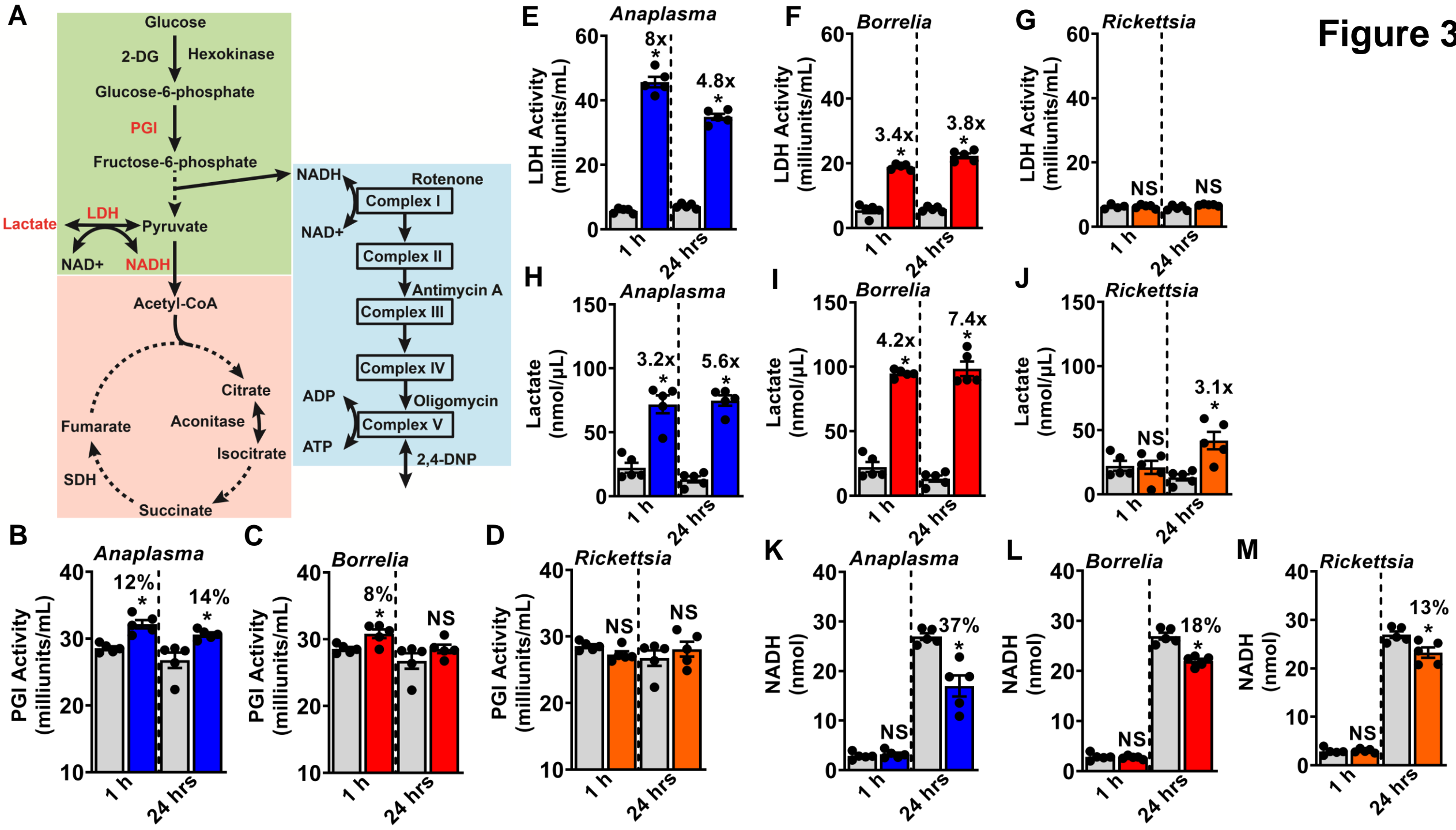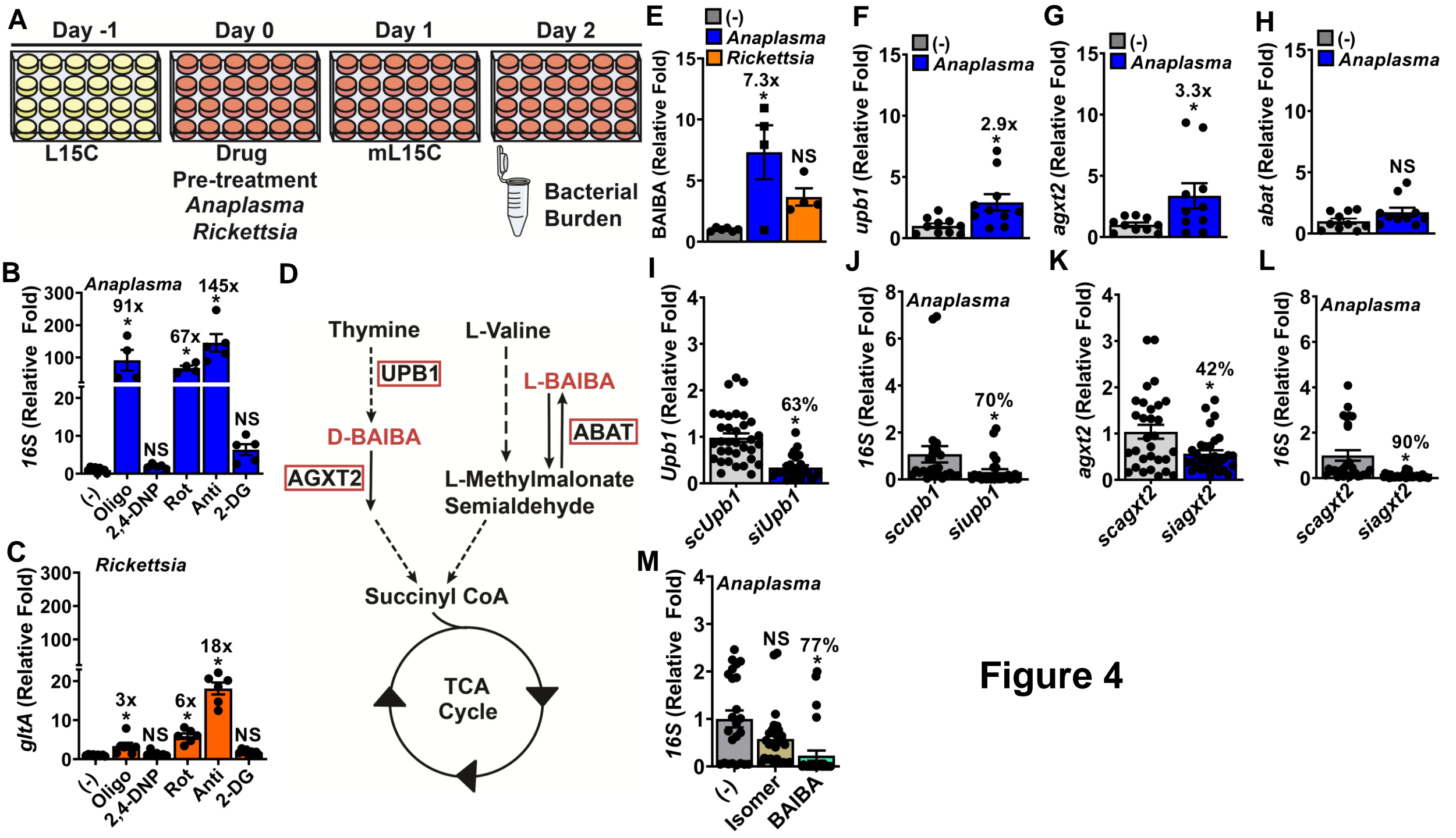708   LC/MS metabolomics data into chemical libraries. *Journal of Cheminformatics* **2**, 9
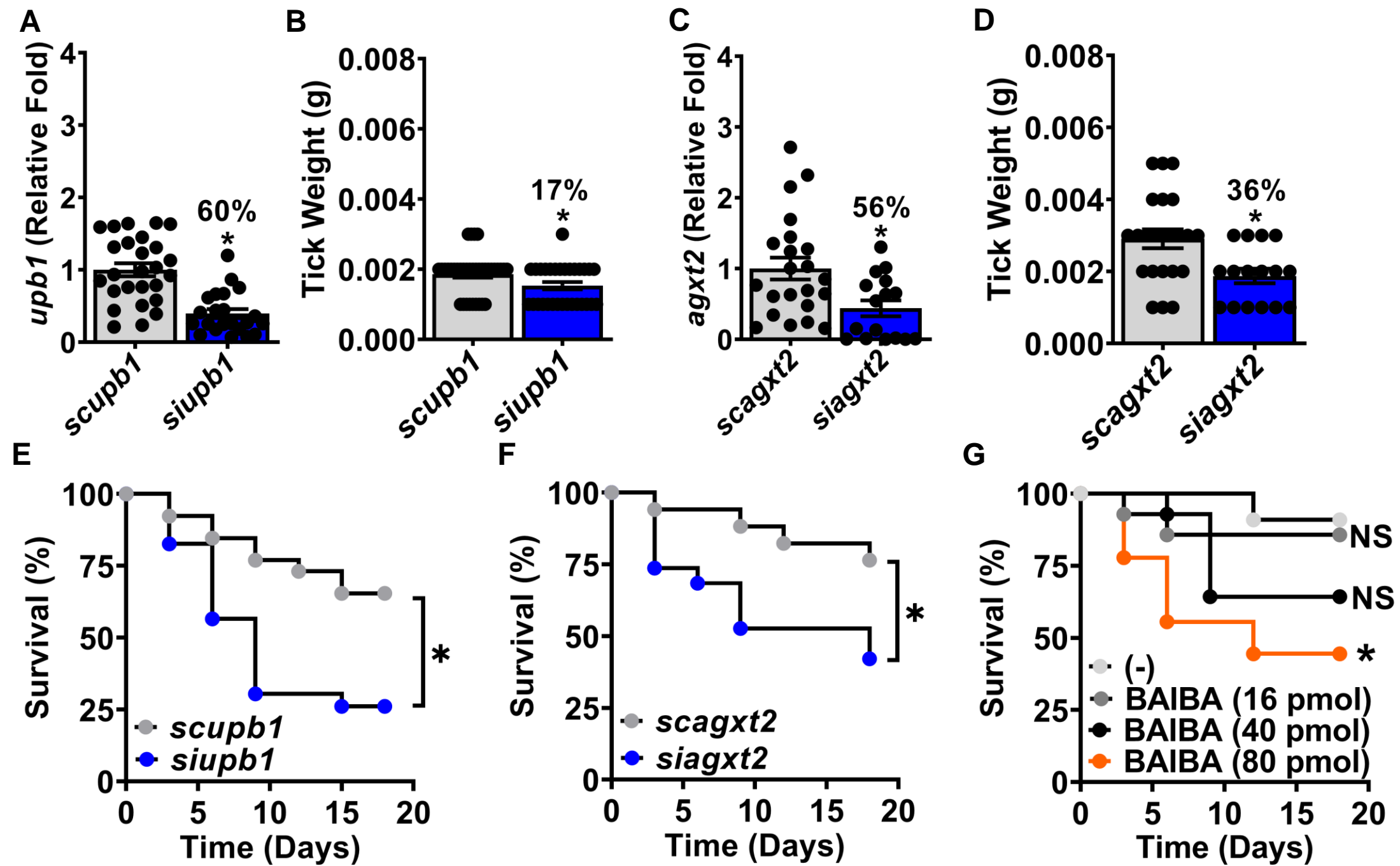
709   (2010).

710

Figure 1

Figure 2

Figure 3

Figure 4

Figure 5